

# Synthesis of NiO Nanoparticles: Effect of Method on Structural Properties of NiO Nanoparticles

Samaneh Pirzad Ghias Abadi, Mahmood Borhani Zarandi\* and Naser Jahanbakhshi Zadeh

Department of Physics, Yazd University, Yazd, Iran

(\*) Corresponding author: mborhani@yazd.ac.ir

(Received: 10 December 2021 and Accepted: 12 April 2022)

## Abstract

This work synthesized NiO nanoparticles by chemical precipitation and thermal decomposition methods at different annealing temperatures. The properties of synthesized nanopowders were compared by X-ray diffraction (XRD), scanning electron microscopy (SEM), and Fourier transformed infrared (FT-IR). The X-ray diffraction pattern analysis indicated that samples annealed at 300 °C and 600 °C have face-centered cubic (fcc) with lattice parameter  $a = 4.17960 \text{ \AA}$  and hexagonal structures with lattice parameters  $a=b= 2.95 \text{ \AA}$ ,  $c=7.23 \text{ \AA}$ , respectively. Also, by increasing annealing temperature, the crystallinity and size of NiO nanoparticles have increased, and samples synthesized by the chemical precipitation method have a smaller size than other samples. For 600 °C calcination temperature and compared to other methods, XRD pattern of samples synthesized by thermal decomposition method showed higher intensity of peaks which resulted in larger nanoparticles. FT-IR results confirmed the formation of NiO nanoparticle composition. Also, the FT-IR spectrum of samples synthesized with different methods and varying annealing temperatures didn't change significantly. This enhanced chemical understanding is paramount for the rational control of synthesizing NiO and its applications in electronic and electro-optical research.

**Keywords:** Nickel oxide, Nanoparticle, Structural properties, Chemical precipitation, Thermal decomposition.

## 1. INTRODUCTION

Nanoparticles have special electronic, magnetic, optical and catalytic properties in comparison with their bulk structure [1-6]. There are several methods for synthesizing nanoparticles. Depending on the method chosen for synthesis, the resulting nanoparticles can have different applications [7-12]. Nickel Oxide (NiO) is a p-type semiconductor because of vacancy in  $\text{Ni}^{2+}$  sites [13, 14]. NiO nanoparticles have a usage in antiferromagnetic layer [15], p-type transparent conducting films [16], electrochromic devices [17, 18], gas sensors [19], catalyst [20] and perovskite solar cells [21, 22]. NiO nanopowders synthesize by different mechanical and chemical methods. The Chemical methods include: sol gel [23], low-pressure spray

pyrolysis [24, 25], simple liquid phase process [26], hydrothermal [27] and chemical precipitation [28]. Reduction of synthesis costs is one of the main purposes of synthesizing NiO nanoparticles. Wardani et al. synthesized NiO nanoparticles using Ageratum conyzoides L. leaf extract via green route for catalytic activity [29]. They showed that the catalytic activity percentage of NiO-NP shown 83% in the reduction of methylene blue dye compared with catalytic activity sans catalyst was 28%. Kim demonstrated a facile polyethylene glycol (PEG)-assisted sol-gel synthesis of the compact NiO layer as the hole-selective layer in perovskite solar cell [30]. His study revealed that the compact NiO layer assisting better interfacial characteristics for favorable

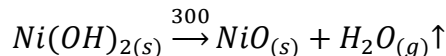
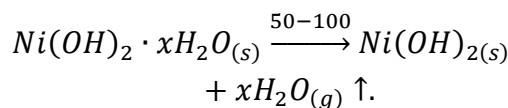
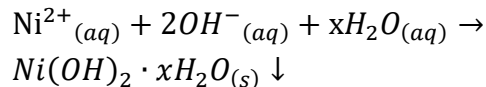
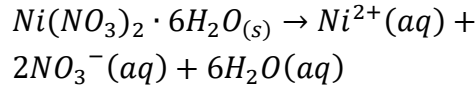
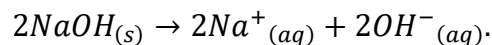
charge transport and promotes all the parameters determining the power conversion efficiency of solar cell. Miao et al. synthesized NiO flake-flower architectures via hydrothermal method for the gas sensing applications [31]. These results demonstrated that gas sensor based the flower-like NiO was highly sensitive and selective for ethanol vapor. Bahari et al. [32] prepared NiO nanoparticles by chemical precipitation and using three different surfactants. Their results showed poly ethylene glycol was more effective in reducing nanoparticles size than other surfactants. Still, they didn't study the effect of surfactant and calcination temperature on samples' phase structure and chemical composition. Khani et al. [33] synthesized NiO nanoparticles with spherical morphology using the thermal decomposition method. The particle size average was 26 nm and 46 nm at 350°C and 650°C calcination temperatures, respectively. They didn't study the effect of calcination temperature on phase structure and chemical composition of NiO nanoparticles. Nickel nitrate, nickel chloride and nickel acetate are the major precursors for synthesis of NiO nanoparticles. Nickel chloride and nickel acetate are the most used and highly available precursors. Unlike nickel acetate and nickel chloride precursors corrode the deposition equipment [34]. Accordingly, in this work, nickel nitrate was selected as a precursor for the synthesis of nanoparticles via different chemical methods. Then, structural properties of these nanoparticles were compared with each other. We studied the effect of calcination temperature and the type of surfactant on phase structure and chemical composition of nanoparticles, while in previous research this was not done.

## 2. EXPERIMENTAL

### 2.1. Synthesis of NiO Nanoparticles by Chemical Precipitation Method

NiO nanoparticles were synthesized by chemical precipitation [32]. The materials

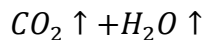
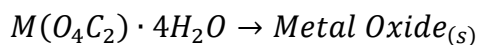
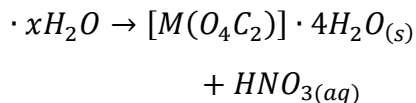
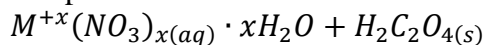
used in this section are nickel nitrate hexahydrate ( $\text{Ni}(\text{NO}_3)_2 \cdot 6\text{H}_2\text{O}$ ) (as a precursor), sodium hydroxide ( $\text{NaOH}$ ) (as precipitator) and polymeric surfactants for the reduction in particles size (polyvinylpyrrolidone (PVP MW=65000)), polyethylene glycol (PEG, MW=6000). Briefly, 8.70 g of nickel nitrate was dissolved in 60 ml of deionized water. Then, 3 g sodium hydroxide was dissolved in this section we aim to present our main in 150 ml of deionized water. 1 g PVP and PEG as a surfactant were added to the second solution in two different experiments. The former solution was added to the later solution. The obtained solution was stirred by magnetic stirring and filtered and washed with deionized water. The resultant solution was calcined at 300 and 600 °C for 2h. The most important reactions of this synthesis method are:



### 2.2. Synthesis of NiO Nanoparticles by Thermal Decomposition Method

NiO nanoparticles were synthesized by the thermal decomposition method [33]. The materials used in this part were nickel nitrate hexahydrate ( $\text{Ni}(\text{NO}_3)_2 \cdot 6\text{H}_2\text{O}$ ) (as a precursor) and oxalic acid (as precipitator). Briefly, 2.46 g nickel nitrate hexahydrate was dissolved in 20 ml ethanol. This solution was transferred to double opening distillation balloons while the solution was

stirred at 50°C for 1h. In order to obtain nickel oxalate complex, 1.89 g oxalic acid was added to the solution quickly, and the system was in reflux conditions for 3h. The resultant green viscous gel was dried at 80°C and calcined at 300°C and 600°C for 2 h. In this method, total reactions for decomposition of Metal Oxalate compounds are:



### 3. RESULTS AND DISCUSSION

The X-ray diffraction was taken using Bruker's diffractometer model D8 advance. The X-ray source was KαCu with a 1.54 Å° wavelength. Figures 1 and 2 show the XRD patterns of the NiO nanoparticles synthesized by chemical precipitation (using PEG and PVP as surfactant) and the thermal decomposition method calcined at 300°C and 600°C respectively. NiO has an amorphous and crystalline structure. Depending on the mechanism used for synthesize and also growth conditions, different types of crystal structure have been identified for nickel oxide. Figure 1 with calcination temperature of 300°C, shows crystal structure of the face center cubic (fcc) with lattice parameter  $a=4.17960 \text{ \AA}$ . Figure 2 with calcination temperature of 600 °C, shows hexagonal crystal structure with lattice parameters  $a=b=2.95 \text{ \AA}$ ,  $c=7.23 \text{ \AA}$ . This results is compatible with standard cards JCPDS and the works of others [16,17]. Crystallographic planes such as (111), (200), and (220) have appeared, which belong to NiO cubic and hexagonal structures for samples calcined at 300°C and 600°C, respectively.

The particle size (D) was calculated by using Scherer's formula [35]:

$$D = \frac{0.9\lambda}{\beta \cos\theta} \quad (1)$$

$\lambda$  is the wavelength of the X-rays used,  $\beta$  is the full width at half maximum (FWHM) and  $\theta$  is the diffraction angle. The calculated particles sizes are presented in Table 1.

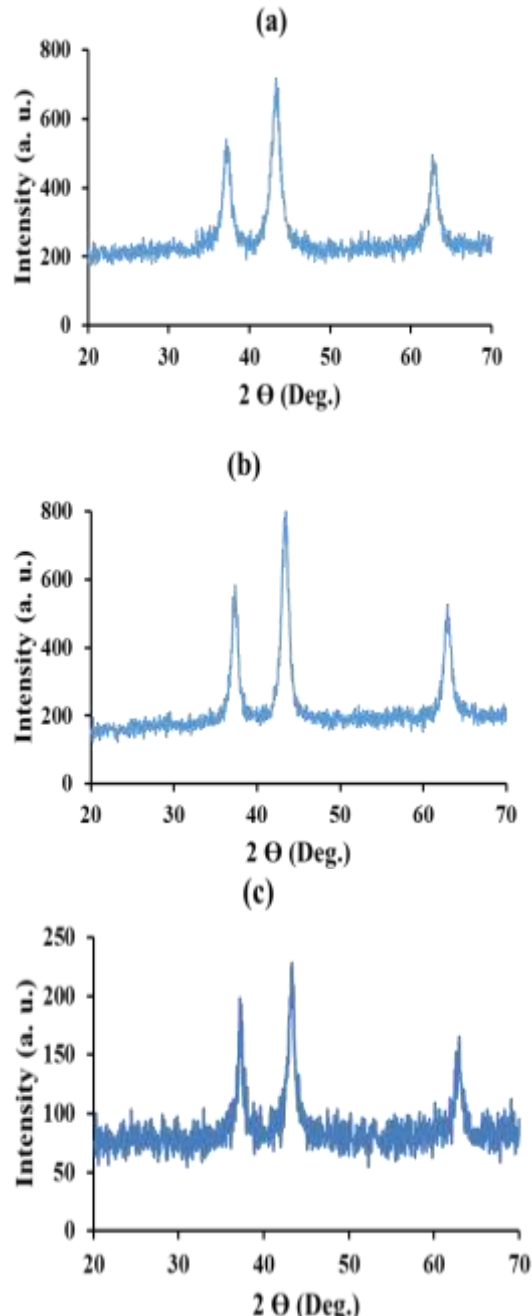


**Figure 1.** XRD patterns of calcined powder at 300°C (a) chemical precipitation (PEG), (b) chemical precipitation (PVP), (c) thermal decomposition.

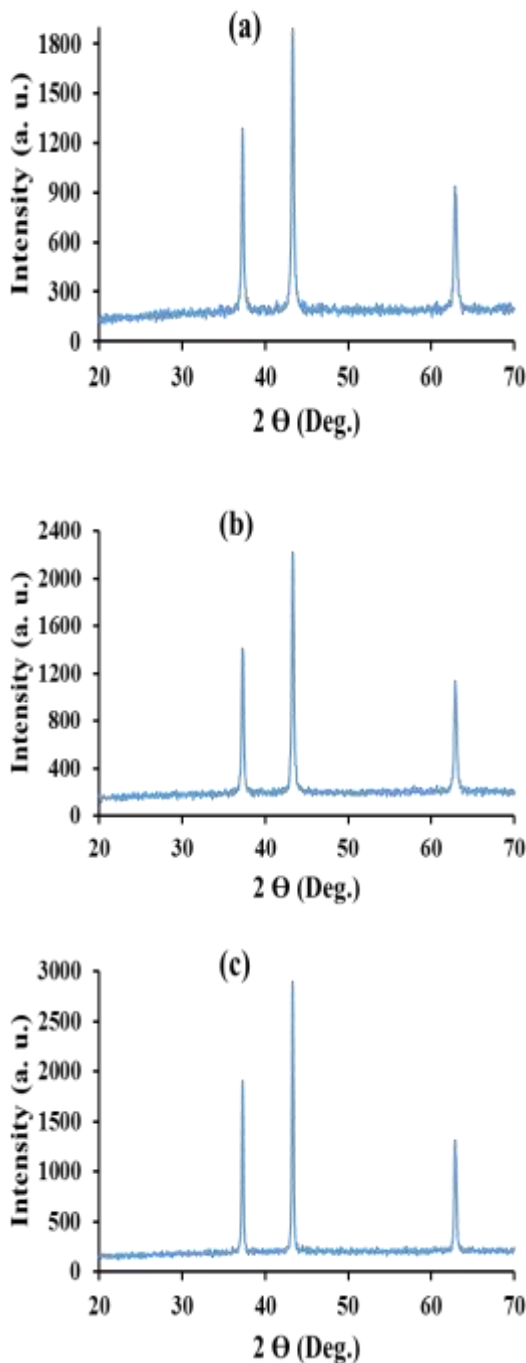


**Figure 2.** XRD patterns of calcined powder at 600°C (a) chemical precipitation (PEG), (b) chemical precipitation (PVP), (c) thermal decomposition.

Figure 2 shows sharper and more intensive diffraction peaks compared to Figure 1. This increment in the intensity of peaks is more considerable in the sample synthesized by the thermal decomposition method, leading to larger particle size [36]

and high crystallinity at 600°C calcination temperature.

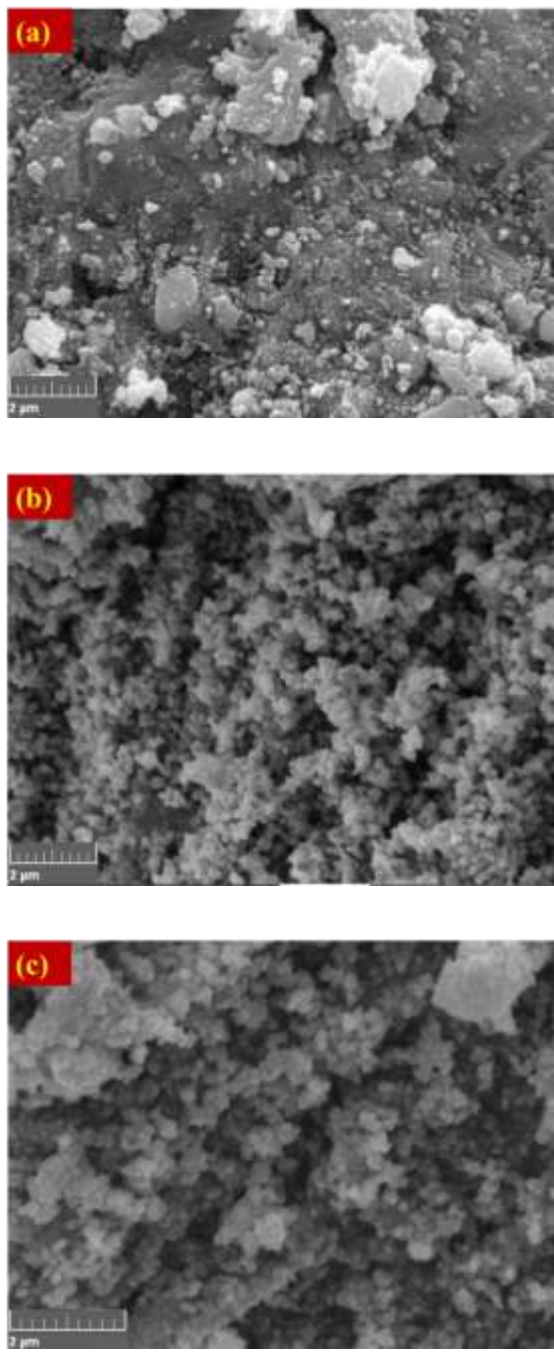
**Table 1.** Particle size and full width at half maximum ( $\beta$ ) for calcined powder at 300 and 600°C.

synthesis method	(hkl)	$\beta$ (deg.)		D(nm)	
		Calcine d at 300°C	Calcine d at 600°C	Calcine d at 300°C	Calcine d at 600°C
chemical precipitation (PEG as surfactant)	(111)	0.925	0.197	9.1	42.6
	(200)	1.246	0.246	6.8	34.7
	(220)	0.987	0.344	9.7	27.0
chemical precipitation (PVP as surfactant)	(111)	0.862	0.246	9.7	34.1
	(200)	0.977	0.246	8.8	34.7
	(220)	0.906	0.296	10	31.5
Thermal decomposition	(111)	0.423	0.226	20	38.5
	(200)	0.637	0.236	13.4	36.4
	(220)	0.740	0.314	12.6	30.1

Also, the appearance of low-intensity peaks in Figure 1 maybe due to an incomplete reaction, so increasing in annealing temperature eliminates these peaks (Figure 2). According to table 1, NiO nanoparticles size synthesized by chemical precipitation is less than other samples at both calcination temperatures.

Figure 3 shows the scanning electron microscopy (SEM) image of the NiO nanopowders taken using TESCAN, Vega 3.

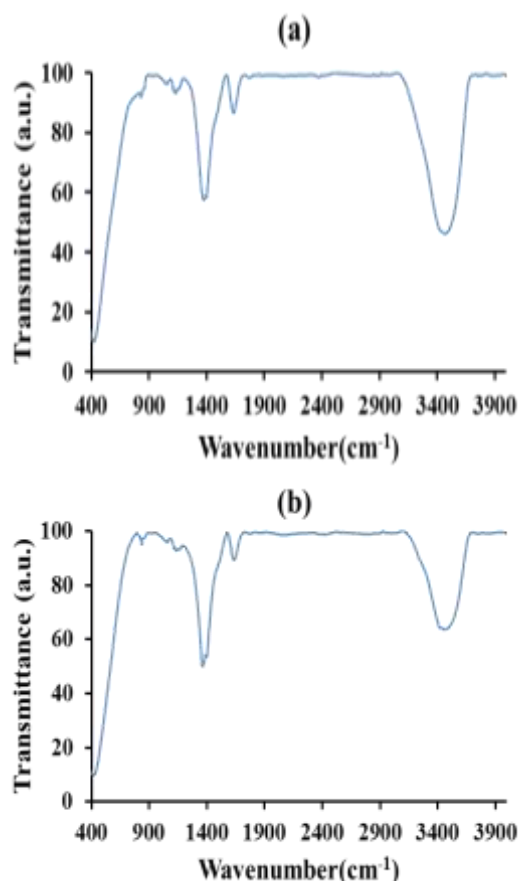
According to Figure 3(b), the sample synthesized by chemical precipitation (PVP as surfactant) has a spherical morphology and a more uniform distribution than the other samples. In two different samples in some areas, agglomeration and less uniformity are observed (Figures 3(a) and 3(c)).



**Figure 3.** The SEM image of NiO nanoparticles were annealed at 600°C. (a) chemical precipitation (PEG), (b) chemical precipitation (PVP), (c) thermal decomposition.

Figure 4 and Figure 5 show the FT-IR transmission spectrum taken on Perkin Elmer- Spectrum RX infrared spectrometer in the range of 400-4000 cm<sup>-1</sup> at room temperature; samples calcined at 300°C and 600°C, respectively. As indicated in

the spectrum, peaks centered at about 400 cm<sup>-1</sup> correspond to Ni-O stretching vibration bands [33]. According to Figure 4, the banding vibrations of samples are almost the same; only the c-o absorption bond in the sample synthesized by thermal decomposition wasn't observed. The absorption peaks have increased for all samples annealed at 600°C (Figure 5). As shown in Figure 5, banding vibrations in all samples are almost the same. These results indicate that different synthesis methods and increasing calcination temperature don't affect the chemical composition samples [28]. Also, all important bonds from the FT-IR spectrum for NiO nanopowders with different synthesis methods and annealing temperatures are summarized in Tables 2 and 3 [33, 37]. According to these tables, absorption peaks observed in IR spectrum indicate the banding vibration of ionic CO<sub>3</sub><sup>2-</sup>. This indicates the fact that NiO nanoparticles tend to absorb carbonate ions [30, 33].



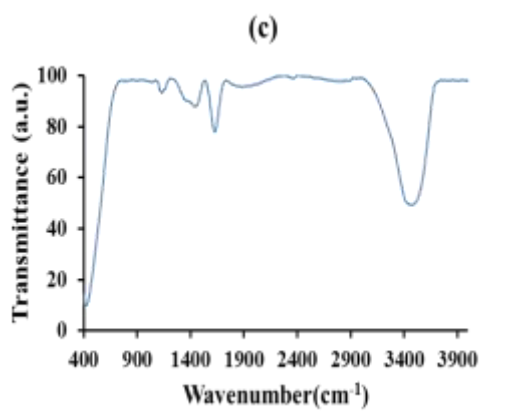


**Figure 4.** FT-IR spectroscopy of NiO nanoparticles synthesized by a) chemical precipitation (PEG), (b) chemical precipitation (PVP), and (c) thermal decomposition. All samples were annealed at 300°C.

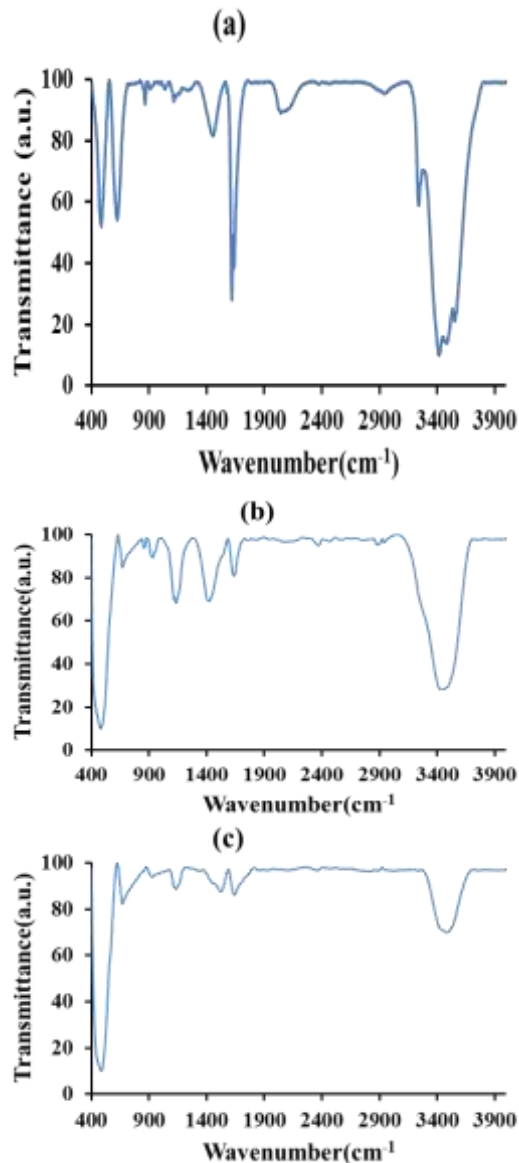


**Figure 5.** FT-IR spectroscopy of NiO nanoparticles synthesized by SEM image of a) chemical precipitation (PEG), (b) chemical precipitation (PVP), and (c) thermal decomposition (Reflux). All samples were annealed at 600°C.

**Table 2.** The assignments of the most important bonds in the FT-IR spectra of NiO nanoparticles annealed at 300°C

synthesis method	wavenumber	Relevant bond
chemical precipitation (PEG as surfactant)	430	O-Ni
	810	O-C
	1134.49,1376.13,1392.87	$CO_3^{2-}$
	1633.13	H-O-H
	3466.68	H-O
chemical precipitation (PVP as surfactant)	424	O-Ni
	835.78	O-C
	1364.10,1397.26	$CO_3^{2-}$
	1635.13	H-O-H
	3465.72	H-O
thermal decomposition	432.10	O-Ni
	1134.15, 1442.26, 1112.32	$CO_3^{2-}$
	1626.06	H-O-H
	3469.96	H-O

#### 4. CONCLUSION

NiO nanoparticles were synthesized by chemical precipitation (using PEG and PVP as surfactant) and thermal decomposition methods, using nickel nitrate hexahydrate as a precursor and calcination temperatures at 300°C and 600°C. XRD analysis showed that samples calcined at 300°C are in the cubic phase with lattice parameter  $a = 4.17960 \text{ \AA}$  and samples annealed at 600°C are in the hexagonal phase with lattice parameters  $a=b=2.95 \text{ \AA}$ ,  $c=7.23 \text{ \AA}$ . Nanoparticles' size has increased with an increase in annealing temperature. According to the XRD patterns, the crystallinity of NiO nanoparticles that calcined at 600 °C was higher than samples calcined at 300 °C.

**Table 3.** The assignments of the most important bonds in the FT-IR spectra of NiO nanoparticles annealed at 600°C

synthesis method	wavenumber	Relevant bond
chemical precipitation (PEG as surfactant)	485.79	O-Ni
	624.38	H-O-Ni
	865.80	O-C
	1114.17, 1453.88	$CO_3^{2-}$
	1617.96, 1637.83	H-O-H
	2042.05, 2940.25	C-H
	3238.51, 3415.87, 3548.67	H-O
chemical precipitation (PVP as surfactant)	481.74	O-Ni
	670.15	H-O-Ni
	854.71	O-C
	1116.71, 1136.23, 1419.73	$CO_3^{2-}$
	1635.74	H-O-H
	2370.85, 2884.06, 2931.86	H-C
	3424.24	H-O
thermal decomposition	485.95	O-Ni
	669.80	H-O-Ni
	1135.61	$CO_3^{2-}$
	1640.39	H-O-H
	3485.13	H-O

Also, NiO nanoparticles synthesized by thermal decomposition have a larger size than other samples. Size of NiO nanoparticles synthesized by chemical precipitation is less than other samples at both calcination temperatures (300 and 600 °C). SEM images confirmed that NiO nanoparticles have a spherical shape. FT-IR analysis verified the formation of NiO nanoparticle composition. Changing the synthesis method and increasing in calcination temperature doesn't change the chemical composition of the NiO nanopowders significantly.

## ACKNOWLEDGEMENT

The authors wish to thank the Yazd photonics research group (YPRG) of Yazd University.

## CONFLICT OF INTEREST

The authors declare that they have no conflict of interest.

## REFERENCES

1. Halomoan, I., Yulizar, Y., Surya, R. M., Apriandanu, D. O. B., "Facile preparation of CuO-Gd<sub>2</sub>Ti<sub>2</sub>O<sub>7</sub> using Acmella uliginosa leaf extract for photocatalytic degradation of malachite green", *Materials Research Bulletin*, 150 (2022) 111726.
2. Elviera, E., Yulizar, Y., Apriandanu, D. O. B., Surya, R. M., "Fabrication of novel SnWO<sub>4</sub>/ZnO using Muntingia calabura L. leaf extract with enhanced photocatalytic methylene blue degradation under visible light irradiation", *Ceramics International*, 48 (2022) 3564-3577.
3. Aquisman, A. E., Wee, B. S., Chin, S. F., Kwabena, D. E., Michael, K. O., Bakeh, T., Semawi, Sh., Sylvester, D. S., "Synthesis, Characterization, and Antibacterial Activity of ZnO Nanoparticles from Organic Extract of Cola Nitida and Cola Acuminata Leaf", *International Journal of Nanoscience and Nanotechnology*, 16 (2020) 73-89.
4. Yulizar, Y., Gunlazuardi, J., Apriandanu, D. O. B., Syahfitri, T. W. W., "CuO-modified CoTiO<sub>3</sub> via Catharanthus roseus extract: A novel nanocomposite with high photocatalytic activity", *Materials Letters*, 277 (2020) 128349.
5. Zadeh, N. J., Zarandi, M. B., Nateghi, M. R., "Optical properties of the perovskite films deposited on mesoporous TiO<sub>2</sub> by one step and hot casting techniques". *Thin Solid Films*, 671 (2019) 139-146.
6. Zadeh, N. J., Zarandi, M. B., Nateghi, M. R., "The Effect of Phase of Alumina on Crystallinity of Perovskite Layer in Perovskite Solar Cells", *Iranian Journal of Crystallography and Mineralogy*, 26 (2018) 789-796.
7. Yulizar, Y., Eprasaty, A., Apriandanu, D. O. B., Yunarti, R. T., "Facile synthesis of ZnO/GdCoO<sub>3</sub> nanocomposites, characterization and their photocatalytic activity under visible light illumination", *Vacuum*, 183 (2021) 109821.
8. Apriandanu, D. O. B., Yulizar, Y., "Tinospora crispa leaves extract for the simple preparation method of CuO nanoparticles and its characterization", *Nano-Structures & Nano-Objects*, 20 (2019) 100401.
9. Rathinamala, I., Saranya, A., Jeyakumaran, N., Prithivikumaran, N., "Sol – Gel Spin Coated Cadmium Sulphide Thin Films on Silicon (1 0 0) Substrates for Optoelectronic Applications", *International Journal of Nanoscience and Nanotechnology*, 13 (2017) 159-167.
10. Bioki, H. A., Zarandi, M. B., "ZnS Nanoparticles Effect on Electrical Properties of Au/PANI-ZnS/Al Heterojunction", *International Journal of Nanoscience and Nanotechnology*, 15 (2019) 45-53.

11. Yulizar, Y., Abdullah, I., Surya, R. M., Parwati, N., Apriandanu, D. O. B., "Two-phase synthesis of NiCo<sub>2</sub>O<sub>4</sub> nanoparticles using Bryophyllum pinnatum (Lam) Oken leaf extract with superior catalytic reduction of 2,4,6-trinitrophenol", *Materials Letters*, 311 (2022) 131465.
12. Zadeh, N. J., Zarandi, M. B., "Interfacial engineering of mp-TiO<sub>2</sub>/CH<sub>3</sub>NH<sub>3</sub>PbI<sub>3</sub> with Al<sub>2</sub>O<sub>3</sub>: Effect of different phases of alumina on performance and stability of perovskite solar cells", *Journal of Materials Research*, 36 (2021) 4938–4950.
13. Bidoult, O., Maglione, M., Kchikech, M., "Polaronic relaxation in perovskite", *Phys. Rev.*, 89 (1995) 4195.
14. Wu, J., Nan, C.W., Lin, Y., Deng, Y., "Giant Dielectric Permittivity Observed in Li and Ti Doped NiO", *Phys. Rev.*, 89 (2002) 217601.
15. Fujii, E., Tomozawa, A., Torii, H., Takayama, R., "Preferred orientation of NiO Films Prepared by Plasma Enhanced Metal organic Chemical Vapor Deposition", *Jpn. J. Appl. Phys.*, 35(1996) 1801-1803.
16. Sato, H., Minami, T., Takata, S., Yamada, T., "Transparent conducting p-type NiO thin films prepared by magnetron sputtering", *Thin Solid Films*, 236 (1993) 27.
17. Wei, Y., Chen, M., Liu, W., Li, L., Yan, Y., "Electrochemical investigation of electrochromic devices based on NiO and WO<sub>3</sub> films using different lithium salts electrolytes", *Electrochimica Acta*, 247(2017) 107-115.
18. Wen Chen, P. C., Chang, T., Ko, T., Hsu, S., Li, K., Wu, J., "Fast response of complementary electrochromic device based on Wo<sub>3</sub>/NiO electrodes", *Scientific reports*, 10 (2020) 8430-8442.
19. Deng, X., Zhang, L., Guo, J., Chen, Q., J. Ma, J., "ZnO enhanced NiO-based gas sensors towards ethanol", *Materials Research Bulletin*, 90 (2017) 170-174.
20. Alnarabiji, M. S., Tantawi, O., Ramli, A., Zabidi, N. A. M., Ghanem, O. B., Abdullah, B., "Comprehensive review of structured binary Ni-NiO catalyst: Synthesis, characterization and applications", *Renewable and Sustainable Energy Reviews*, 114 (2019) 109326.
21. Abadi, S. P. G., Zadeh, N. J., Zarandi, M. B., "Synthesis methods of NiOx nanoparticles and its effect on hole conductivity and stability of n-p perovskite solar cells", *Synthetic Metals*, 289 (2022) 117115.
22. Zadeh, N. J., Zarandi, M. B., Nateghi, M. R., "Effect of crystallization strategies on CH<sub>3</sub>NH<sub>3</sub>PbI<sub>3</sub> perovskite layer deposited by spin coating method: dependence of photovoltaic performance on morphology evolution", *Thin Solid Films*, 660 (2018) 65-74.
23. Zorkipli, N. N., Kaus, A. C., Mohamad, M. A. Z., "Synthesis of NiO Nanoparticles through Sol-gel Method", *Procedia Chemistry*, 19 (2016) 626-63.
24. Ukoba, K. O., Eloka-Eboka, F. L., "Review of nanostructured NiO thin film deposition using the spray pyrolysis technique", *Renewable and Sustainable Energy Reviews*, 82 (2018) 2900-2915.
25. Lenggoro, I. W., Itoh, Y., Iida, N., Okuyama, K., "Control of size and morphology in NiO particles prepared by a low-pressure spray pyrolysis", *Materials Research Bulletin*, 38 (2003) 1819-1827.
26. Wang, C. B., Gau, G. Y., Gau, S. J., Tang, C. W., J. L. Bi, "Preparation and characterization of nanosized nickel oxide", *Catalysis Letters*, 101 (2005) 241-247.
27. S. Cao, L. Peng, T. Han, B. Liu, D. Zhu, C. Zhao, J. Xu, Tang, Y., Wang, J., He, S., "Hydrothermal synthesis of nanoparticles- assembled NiO microspheres and their sensing properties", *Physica E: Low-dimensional Systems and Nanostructures*, 118 (2020) 113655.
28. Yin, X., Chen, P., Que, M., Xing, Y., Que, W., Niu, C., Shao, J., "Highly Efficient Flexible Perovskite Solar cells Using Solution- Derived NiO Hole Contacts", *ACSNANO*, 10 (2016) 3630-3636.
29. Wardani, M., Yulizar, Y., Abdullah, I., Apriandanu, D. O. B., "Synthesis of NiO nanoparticles via green route using Ageratum conyzoides L. leaf extract and their catalytic activity", *IOP Conf. Ser.: Mater. Sci. Eng.*, 509 (2019) 012077.
30. Kim, J. K., "PEG-assisted Sol-gel Synthesis of Compact Nickel Oxide Hole-Selective Layer with Modified Interfacial Properties for Organic Solar Cells", *Polymers*, 11 (2019) 120.
31. Miao, R., Zeng, W., Gao Q., "SDS-assisted hydrothermal synthesis of NiO flake-flower architectures with enhanced gas-sensing properties", *Applied Surface Science*, 384 (2016) 304–310.
32. BahariMollaMahaleh, Y., Sadrnezhad, S. K., Hosseini, D., "NiO Nanoparticles Synthesis by Chemical Precipitation and Effect of Applied Surfactant on Distribution of Particle Size", *Journal of Nanomaterials* (2008) 470595.
33. Khani, S., Jafarian, M., "Synthesized of Nickel Oxide Nanostructures via Thermal Decomposition of Nickel Nitrate and Chloride at Low Temperature", *Journal of Nano Materials*, 6 (2015) 221-227
34. Ukoba, K.O., Eloka-Eboka, A.C., Inambao, F.L. "Review of nanostructured NiO thin film deposition using the spray pyrolysis technique", *Renewable and Sustainable Energy Reviews*, 82 (2018) 2900-2915.
35. Cullity, B. D., "Elements of X-ray Diffraction", Addison-Wesley Publishing Co. Inc., New York, (1976).
36. Sharma, R., Acharya, A. D., Moghe, S., Shrivastava, S. B., Gangrade, M., Shripathi, T., Ganesan, V., "Effect of cobalt doping on microstructural and optical properties of nickel oxide thin films", *Materials Science in Semiconductor Processing*, 23 (2014) 42-49.

37. Rahdar, A., Aliahmadi, M., Azizi, Y., "NiO Nanoparticles: synthesis and Characterization", *Journal of Nanostructures*, 5 (2015) 145-151.